Current-Voltage characteristics of the Azo-benzene nano-molecular wires from first principles

H. Aghaie,[a*] M. R. Gholami,[b] M. Monajjemi,[a] S. Yeganegi,[c] M. D. Ganji[a]

[a]Department of Chemistry, Science & Research Campus,Islamic Azad University,Tehran, Iran
[b]Department of Chemistry, Sharif University of Technology, Tehran, Iran
[c]Department of Chemistry, University of Mazandaran, Mazandaran,Babulsar, Iran

Abstract: Using Density Functional Non-Equilibrium Green's Function (DFT-NEGF) method we perform a detailed study of the transport properties of a novel light-driven molecular switch. We consider two isomers of Azo-benzene moleculular wires, *Cis* and *Trans*, sandwiched between two Au (1 0 0) electrodes. It has been found that the conductance of the *cis* isomer is significantly smaller than that of the *trans* one. Thus, whenever the Azo-benzene is made to flip from the *cis* conformation to the *trans* conformation, the wire is predicted to switch from a weakly conducting to a highly conducting state. The transmission coefficients T (E) of the two-probe system at zero bias have also been analyzed.

Keywords: Molecular electronics, Electron transport, DFT-NEGF method, Light-driven nano-switchs, Azo-benzene

Introduction

Organic molecules as functional units for electronic apparatus applications have been attracted more attention because they represent the ultimate miniaturization of electronic systems and a possible goal of nanoelectronics [1-11]. The recent significant advances [1-11] predict a brilliant future for molecular electronics. Electronic devices that switch between high and low resistance states are at the heart of the modern information technology. As miniaturization of this technology continues to progress the long-standing fundamental problem of identifying and understanding the smallest physical systems that are capable of switching behavior is attracting growing interest [3, 8–11]. Switching between *on* and *off* states can be performed by applying an external bias or by using a scanning tunneling microscope tip to manipulate the system [3, 8–11]. However, since these methods impose severe limitations in device applications [8, 9] thus they are not ideal and it is reasonable to find alternative methods, such as those based on fast, light-driven processes. The azo-benzene molecular wire considered here is one such candidate for an optoelectronic device. This novel molecular wire has two conformations, *trans* and *cis,* as represented in Fig. 1. The molecule can switch reversibly from one structure to another under photoexcitation, with the structural change occurring on an electronically excited state [9].

Figure 1. Optimized geometric structures of two isomers of an Azo-benzene molecular wire, (a) *Trans* isomer and (b) *Cis* isomer.

(a)

(b)
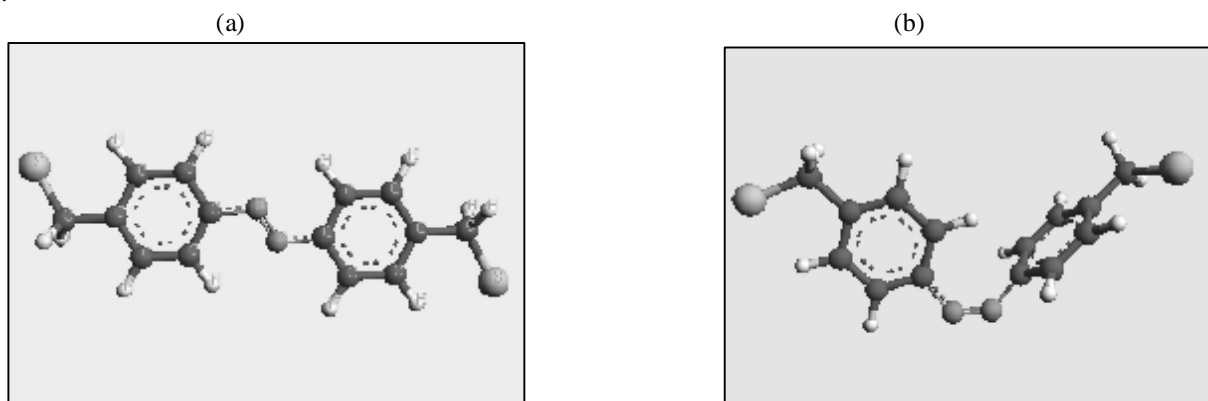
*Corresponding author. Tel: +(98) 9121447819; E-mail: *hn_aghaie@yahoo.com

In the present work, we investigate the electron transport phenomena through the *cis/trans* isomer of an azo-benzene single molecular wire sandwitched between two semi-infinite gold (1 0 0) leads.

Furthermore, the considered molecular wire has been functionalized by replacing a hydrogen ended atom with an S group to provide a good contact with gold electrodes. To contribute to the knowledge about the mechanism of switching behaviour in single molecular devices, in the current research we present a detailed first-principles analysis of the *I–V* characteristics of the azo-benzene molecular wire. The light-driven molecular switch that we describe should be amenable to experimental study with presently available techniques. Thus our findings also raise the prospect of bridging the gap that has persisted in this field between theory and experiment since molecular switching was first observed. The organization of the Letter is as follows. We start with a brief description of the density functional based non-equilibrium Green's function method (Section 2), and in Section 3 we report our main results for the transmission functions of the different structures and discuss their implications, together with an analysis of the molecular levels important for electron transmission. In Section 4, the results are summarized.

Computational details

The calculations have been performed using a recently developed first-principles package SMEAGOL [12, 13], which is based on the combination of DFT (as implemented in the well-tested SIESTA method [14]) with the NEGF technique [15, 16]. SMEAGOL is capable of fully self consistently modeling the electrical properties of nano-scale devices that consist of an atomic scale system coupling with two semi-infinite electrodes. Such nano-scale devices are referred to as two-probe systems and they are divided into three parts for theoretical calculations: left and right electrodes, and a central scattering region. The scattering region actually includes a portion of the semi-infinite electrodes. The simulation procedure of such two-probe systems can be described briefly as follows.

Firstly the electronic structure of two electrodes is calculated only once by SMEAGOL to get a self-consistent potential. This potential will be shifted rigidly relative to each other by the external potential bias and provides natural real space boundary conditions for the Kohn-Sham (K-S) effective potential

of the central scattering region. Then from the Green's function of the central scattering region, it can obtain the density matrix and thereby the electron density. Once the electron density is known, the DFT Hamiltonian matrix, which is used to evaluate the Green's function, can be computed using the above boundary conditions by means of standard methods.

$$\hat{G} = \lim_{d \to 0}[(E + id)\hat{S} - \hat{H}_{S[r]} - \hat{\Sigma}_L - \hat{\Sigma}_R]^{-1} \quad (1)$$

where $\hat{H}_{S[r]}$ is DFT Hamiltonian and $\hat{\Sigma}_L$ and $\hat{\Sigma}_R$ are the self-energies respectively for the left and right lead. This procedure is iterated until self-consistency is achieved. Moreover, the current through the atomic scale system can be calculated from the corresponding Green's function and self-energies using Landauer-Buttiker formula [17]

$$I(V) = \frac{2e}{h} \int_{-\infty}^{+\infty} dE[f_l(E - m_l) - f_r(E - m_r)]T(E,V) \quad (2)$$

Where m_l and m_r are the electrochemical potentials of the left and right electrodes respectively, *i.e.*,

$$m_L - m_R = eV_b \quad (3)$$

and f_r, f_l are the corresponding electron distribution of the two electrodes. $T(E,V)$ is the transmission coefficient at energy E and bias voltage V, which is given by

$$T(E,V) = Tr[\mathrm{Im}\Sigma_l(E)G^R(E)\mathrm{Im}\Sigma_r(E)G^A(E)] \quad (4)$$

where $G^R(E)$ and $G^A(E)$ are the retarded and advanced Green's function of the central region. Based on the eigenchannel decomposition of the conductance, this total transmission $T(E)$ can be decomposed into nonmixing eigenchannels $T_n(E)$ [18] as

$$T(E) = \sum_n T_n(E) \quad (5)$$

In our DFT calculation, the local-density approximation (LDA) to the exchange-correlation potential [19] is used. Only valence electrons are considered in the calculation, and the wave functions are expanded by localized numerical (pseudo)atom orbitals (PAO's) [20]. The atomic cores are described by norm-conserving pseudo potentials [21].

The structural model for our theoretical analysis is illustrated in Fig. 2. In this two-probe system, Azo-

benzene couples with two atomic scale Au (1 0 0) electrodes which extend to reservoirs at ±∞ where the current is collected. Three Au atomic layers have been chosen for the electrode cell in the z-direction. In the central scattering region the Azo-benzene couples with three atomic layers to the left/right side. These atomic layers in the central scattering region are large enough [22] so that the perturbation effect from the scattering region is screened and they are denoted as surface-atomic layers.

Figure 2. A schematic representation of the Azo-benzene molecular wire attached between two Au (1 0 0) electrodes. (a) The ground state of the *trans* isomer, (b) ground state of the *cis* isomer.

(a)

(b)
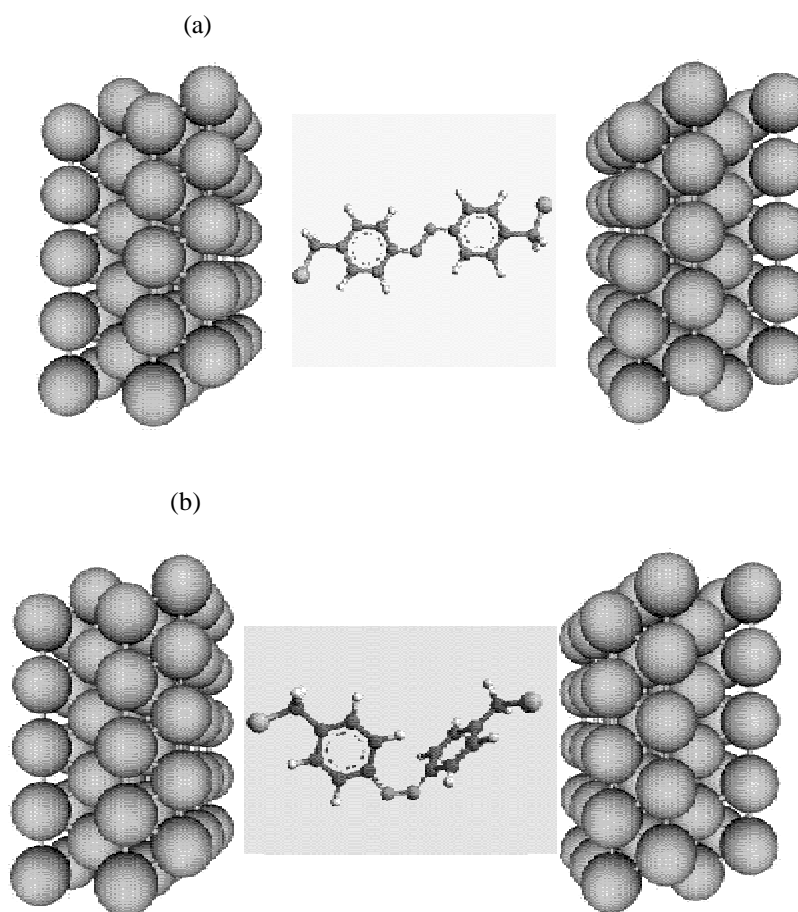
Results and Discussion

The recent theoretical results of electron transport through molecules [20-33] indicate that the current at low bias is carried by molecular orbitals and implies a strong orientation-dependence of the molecular wire's conductance [11, 29]. These effects have been found in semi-empirical [25, 30] and density functional [11, 27] transport calculations. Thus, it is reasonable to expect them to result in a significant change in conductance when two isomers of an Azo-benzene wire which their orbitals are orientated differently, switches between a *cis* and a *trans* conformation, and our calculations show this to be the case. Since DFT-NEGF calculations have been successful in explaining the experimental current-voltage characteristics of a variety molecular wires [30, 31, 33, 34] we adopted this approach here.

In Fig. 3, we show the calculated current of the molecular wire in its ground state conformation for two isomers of the Azo-benzene. It can be seen that the *trans* isomer has a higher current intensity than the *cis* isomer at a bias of about 1.0 V. Thus, whenever the

device is made to flip from a *trans* conformation to a *cis* conformation, by photoexcitation, this molecular wire is predicted to switch from a highly conducting to a weakly conducting state, and vice versa.

Figure 3. Calculated current for the ground state Azo-benzene isomers. At 1.0 V the molecule is in the "*on*" state when the molecule has the *trans* conformation and "*off*" state when the molecule has the *cis* conformation.
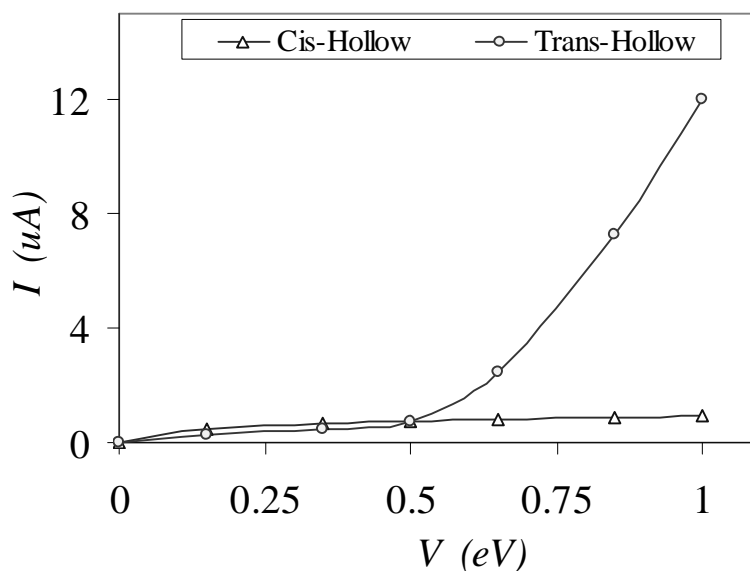
This large difference in conductance between these conformations can be understood within Landauer theory [17] by considering the transmission probabilities, T (E), for electrons to scatter through the molecular wire, taking account of conformational effects. Fig. 4 shows the zero bias transmission spectra of the two-probe systems for both the *cis* and *trans* isomers. They have a region of strong transmission immediately at the Fermi energy, where electrons incident from one of the electrodes can transmit across the molecule to the other electrode significantly. There are specified energy regions where, electrons incident from one of the electrodes can transmit across the Azo-benzene to the other electrode significantly. These energy regions are known as "significant energy regions" (SERs) [35] because incident electrons in these regions contribute most significantly to the transmission spectra. The transmission peaks below the Fermi energy can be attributed to the highest occupied molecular orbitals (HOMO) of the Azo-benzene and those above to the lowest unoccupied molecular orbitals (LUMO). The Fermi energy lies nearest the HOMO, so the onset of current is due to electron transmission through the HOMO. Indeed due to a strong overlap between the first HOMO molecular orbital and the atomic orbitals on the Au atoms.

For *trans* conformation, at zero bias voltage, the HOMO is partly occupied and therefore pinned to the Fermi energy. Hence, due to the charge transfer from the molecule to the gold the molecule becomes slightly positively charged. Consequently there is a strong overlap between the first HOMO molecular orbital and the atomic orbitals of the Au atoms. This results in the strong (broad) transmission due to the first HOMO immediately below the Fermi energy in figure 4 and in the large current value seen for this conformation in figure 3.

Regarding the *cis* conformation, the molecular orbitals are oriented differently and their overlap with the orbitals on the Au surface atoms is weaker. As shown in figure 4 the Fermi energy lies also, nearest the HOMO but, in contrast to the *trans* conformation the transmission spectra is weaker due to the weak overlap between the first HOMO molecular orbital and the atomic orbitals of the gold atoms. This results in the weak transmission due to the first HOMO below the Fermi energy in figure 3 and in the small current value seen for the *cis* conformation in figure 3.

We now show, for the *trans* conformation, that the increases in the current can be understood by studying the changes of coupling between the molecular orbitals in the Azo-benzene and incident states in the electrodes under various external biases. As mentioned above, a

large transmission coefficient indicates a strong coupling between the electrodes and the molecule, and the evolution of transmission curves with external biases can help us understand how the changes of the coupling between the electrodes and molecule determines the *I-V* characteristics in the system. As it can be seen from figure 4 we can divide the whole energy region into two kinds of regions according to whether *T* (E,V) = 0 or not in them [35]. In the regions where *T* (E, V) is not zero, the incident electrons can transmit across the molecule, and they are known as transmission regions. In the other regions where *T* (E, V) is zero, the incident electrons cannot transmit across the molecule, and they are known as transmission intervals [35]. It can be seen that the transmission interval near the Fermi energy under zero bias is broadened by increasing the voltage biases. It can be explained by the relative shift of the energy regions of the left and right electrodes.

As mentioned above the current, *I*, is obtained from

$$I(V) = \frac{2e}{h} \int_{-\infty}^{+\infty} dE[f_l(E - m_l) - f_r(E - m_r)]T(E,V) \quad \text{where}$$

μ_L and μ_R are the electrochemical potentials of the left/right electrodes. The region between μ_L and μ_R is

called the bias window or integral window [35], as delimited in figure 4 with the vertical dashed lines. Thus, the current is determined by *T* (E, V) in the bias window and is further only determined by the transmission regions in the bias window because *T* (E, V) is zero in the transmission interval and has no contribution to the current.

It can be seen also from figure 4 that with the external bias increasing from 0.0V to 1.0 V, the new transmission region broadens rapidly since the electrons in the higher energy regions of the left electrode can transmit across the molecule to the lower energy regions of the right electrode in an increasingly wider energy region. As a result, the broadened transmission coefficient spectrum indicates a strong coupling between the molecular orbitals in the Azo-benzene and the incident states from the electrodes, thus the current increases with increases of the bias voltage. Thus, we arrive at the prediction that a wire as simple as Azo-benzene can be made to switch through its interaction with a suitable electrode. The *on* state corresponds to the *trans* isomer of the Azo-benzene, whereas *off* state corresponds to the *cis* isomer.

Figure 4. Transmission function under zero bias as function of the injection energy of electron of the isomers of the Azo-benzene wires coupled to Au (1 0 0) electrodes. The solid curves indicate *T (E)* of the *trans*-Azo-benzene while the dashed curves represent the *T (E)* of the *cis*-Azo-benzene. All energy is relative to the Fermi energy of the electrode.
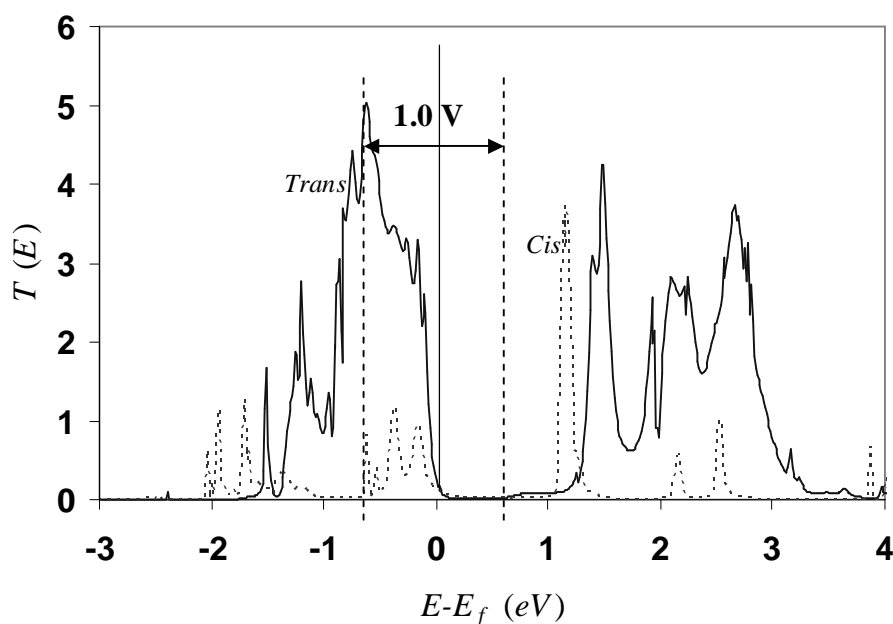
Conclusion

We investigated the *I-V* characteristics of a novel light-driven molecular switch by Density Functional Non-Equilibrium Green's Function method, and presented a realistic theory of its switching behaviour. We considered two isomers of the Azo-benzene molecular wire sandwiched between two Au (1 0 0) electrodes. We found that *trans* conformation of the two-probe system show highly conducting, *on* condition, at around 1.0 V while the *cis* conformation show weakly conducting, *off* condition, there. Thus, whenever the Azo-benzene is made to flip from the *cis* conformation to the *trans* conformation, the wire is predicted to switch from a weakly conducting to a highly conducting state. In the *cis* conformation, due to the different orientations of the two π-bonds of the molecule, orbitals on different bonds have different conformations.

The transmission coefficients *T* (E) of the two-probe system at zero bias are analyzed, and it suggests that the variation of the coupling between the molecular orbitals with external bias leads to switching behaviour. The switching mechanism that we have introduced here relies on the various orientation of the molecular orbitals in the wire thus should be broadly applicable.

Acknowledgements

References

[1] Joachim, C.; Gimzewski, J. K.; Schlittler, R. R.; Chavy, C. *Phys. Rev. Lett*. **1995**, *74,* 102.

[2] Nikolai, B. Z.; Erbe, A.; Bao, Z.; Weirong, J.; Garfunkel, E. *Nanotechnology* **2005**, *16,* 495.

[3] Moresco, F.; Meyer, G.; Rieder, K. H. *Phys. Rev. Lett*. **2000**, *86,* 672.

[4] Xue, Y.; Datta, S.; Hong, S.; Reifenberger, R.; Henderson, J. I.; Kubiak, C. P. *Phys. Rev*. B **1999**, *59,* R7852.

[5] Taylor, J.; Guo, H.; Wang, J. *Phys. Rev*. B **2001**, *63,* 121104.

[6] Di Ventra, M.; Pantelides, S. T.; Lang; N. D. *Phys. Rev. Lett*. **2000**, *4,* 979.

[7] Lang, N. D. *Phys. Rev*. B **1995**, *52,* 5335.

[8] Seminario, J. M.; Derosa, P. A.; Bastos, J. L. *J. Am. Chem. Soc*. **2001**, *124,* 10266.

[9] Zhang, C.; Du, M. H.; Cheng, H. P.; Zhang, X. G.; Roitberg, A. E.; Krause, J. L. *Phys. Rev. Lett*. **2004**, *92,* 158301.

[10] Yang, F. O.; Xu, H.; Fan, T. *J. Appl. Phys*. **2007**, *102,* 064501.

[11] Ganji, M. D. *Nanotechnology* **2008**, *19,* 025709.

[12] Rocha, A. R.; Garcia-Súarez, V. M.; Bailey, S. W.; Lambert, C. J.; Ferrer, J.; Sanvito, S. SMEAGOL (Spin and Molecular Electronics in an Atomically-Generated Orbital Landscape. www.smeagol.tcd.ie).

[13] Rocha, A. R.; Garcia-Súarez, V. M.; Bailey, S. W.; Lambert, C. J.; Ferrer, J.; Sanvito, S. *Nature Materials* **2005**, *4,* 335.

[14] Soler, J. M.; Artacho, E.; Gale, J. D.; Garcia, A.; Junquera, J.; Ordejon, P.; Sanchez-Portal, D. *J. Phys.: Condens Matter* **2002**, *14,* 2745.

[15] Jauho, A. P.; Wingreen, N. S.; Meir, Y. *Phys. Rev*. B **1994**, *50,* 5528.

[16] Haug, H.; Jauho, A. P.; Quantum Kinetics in Transport and Optics of Semiconductors. Springer-Verlag, Berlin: Heidelberg; 1996.

[17] Buttiker, M.; Imry, Y.; Landauer, R.; Pinhas, S. *Phys. Rev*. B **1985**, *31,* 6207.

[18] Brandyge, M.; Surensen, M. R.; Jacobsen, K. W. *Phys. Rev*. B **1997**, *56,* 014956.

[19] Perdew, J. P.; Zunger, A. *Phys. Rev*. B **1981**, *23,* 5048.

[20] Artacho, E.; Suanchez-Portal, D.; Ordejon, P.; Garcia, A.; Soler, J. M. *Phys. Status Solidi* B **1999**, *215,* 809.

[21] Troullier, N.; Martins, J. L. *Phys. Rev*. B **1991**, *43,* 1993.

[22] Roland, C.; Meunier, V.; Larade, B.; Guo, H. *Phys. Rev*. B **2002**, *66,* 035332.

[23] Datta, S.; Tian, W. D.; Hong, S. H.; Reifenberger, R.; Henderson, J. I.; Kubiak, C.P. *Phys. Rev. Lett*. **1997**, *79,* 2530.

[24] Piccinin, S.; Selloni, A.; Scandolo, S.; Car, R.; Scoles, G. *J. Chm. Phys*. **2003**, *13,* 119.

[25] Emberly, E. G.; Kirczenow, G. *Phys. Rev*. B **1998**, *58,* 10911.

[26] Hall, L. E.; Reimers, J. R.; Hush, N. S.; Silverbrook, K. *J. Chem. Phys*. **2000**, *112,* 1510.

[27] Di Ventra, M.; Lang, N. D. *Phys. Rev*. B **2002**, *65,* 045402.

[28] Damle, P. S.; Ghosh, A. W.; Datta, S. *Phys. Rev*. B **2001**, *64,* 201403.

[29] Kornilovitch, P. E.; Bratkovsky, A. M. *Phys. Rev*. B **2001**, *64,* 195413.

[30] Emberly, E. G.; Kirczenow, G. *Phys. Rev. Lett*. **2001**, *87,* 269701.

[31] Stadler, R.; Thygesen, K. S.; Jacobsen, K. W. *Nanotechnology* **2005**, *16,* S155.

[32] Heurich, J.; Cuevas, J. C.; Wenzel, W.; Schon, G. *Phys. Rev. Lett*. **2002**, *88,* 256803.

[33] Kushmerick, J. G.; Holt, D. B.; Yang, J. C.; Naciri, J.; Moore, M. H.; Shashidhar, R. *Phys. Rev. Lett.* **2002**, *89,* 086802.

[34] Athanasopoulos, S.; Bailey, S. W.; Ferrer, J.; Garcya Suarez, V. M.; Lambert, C. J.; Rocha, A. R.; Sanvito, S.; *J. Phys.: Condens Matter* **2007**, *19,* 042201.

[35] Shi, X. Q.; Zheng, X. H.; Dai, Z. X.; Wang, Y.; Zeng, Z. *J. Phys. Chem.* B **2005,** *109*, 3334.